

RESEARCH ARTICLE

[View Article Online](#)
[View Journal](#) | [View Issue](#)



Cite this: *Org. Chem. Front.*, 2025, **12**, 3050

Orthogonal tandem catalysis involving Au(I)-hydroacyloxylation and Rh(I)-hydroformylation reactions†

Ervan Salvi, Roméric Galéa, Camille Van Wesemael, Patrick Wagner, Nicolas Girard* and Gaëlle Blond *

We report an orthogonal tandem catalysis (OTC) involving Au(I)-hydroacyloxylation and Rh(I)-hydroformylation highlighting their compatibility when these metals are employed in a reaction of homogeneous catalysis. Moreover, this OTC allows the synthesis of different carbaldehydes. Several derivatizations were performed at the end of the OTC procedure, giving access to two series of alcohol and oxime derivatives. ^{31}P NMR experiments and kinetic studies carried out on the OTC allowed a detailed understanding of the catalytic cycles involved, highlighting the competitive ligand coordination between the gold and rhodium catalysts.

Received 14th January 2025,
Accepted 24th February 2025

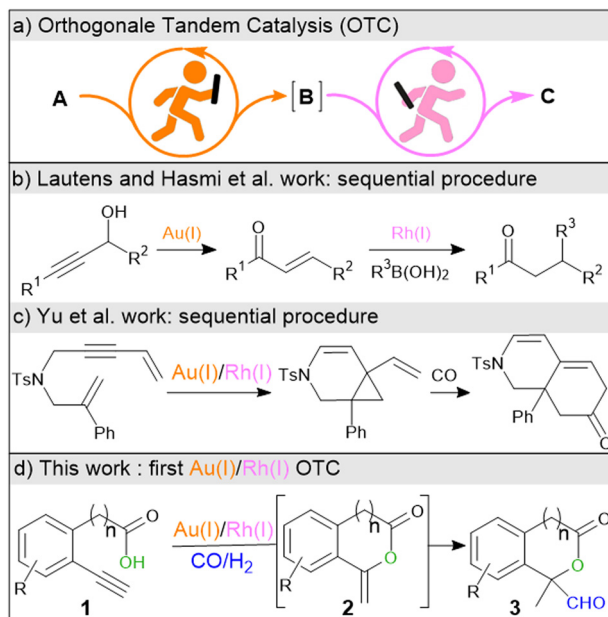
DOI: 10.1039/d5qo00084j

rsc.li/frontiers-organic

Introduction

Since the early 2000s, interest in multi-catalytic reactions in homogeneous media has continued to grow.¹ This is due to the fact that, in nature, biological transformations, often catalyzed, occur sequentially in the same environment. This interest is growing both in academia and in industry.² However, designing such bio-inspired reaction sequences poses a significant challenge for organic chemists. When multiple independent catalytic systems are simultaneously involved in the reaction sequence, these transformations fall into the category of orthogonal tandem catalysis (OTC, Scheme 1a).³ This represents a specific one-pot reaction in which all reactants are present at the beginning of the reaction, unlike classical sequential one-pot reactions, and for which sequential catalytic cycles are carried out without interference between them. OTC reactions caught organic chemists' attention due to the opportunity to build complex systems in which several chemical transformations could be done successively.⁴ The others advantages of OTC reactions over sequential one-pot reactions are manifold: (a) the non-intervention of an operator during the process, (b) the possibility to directly consume intermediate **B** when unstable, (c) avoid poisoning of catalyst by intermediate **B** and (d) promote equilibrium reaction until total

conversion by coupling it directly with the next reaction cycle (thermodynamic leveraging). On the other hand, the conception of such multi-catalytic systems assumes a fine understanding of the catalytic cycles involved because many pitfalls are likely to disrupt the planned chemical mechanics (poisoning of catalysts, interactions between catalysts, solvents and temperatures compatibilities, side reactions, *etc.*).



Université de Strasbourg, Laboratoire d'Innovation Thérapeutique, CNRS UMR 7200, 67000 Strasbourg, France. E-mail: gaelle.blond@unistra.fr, nicolas.girard@unistra.fr

† Electronic supplementary information (ESI) available. CCDC 2384274 and 2111415. For ESI and crystallographic data in CIF or other electronic format see DOI: <https://doi.org/10.1039/d5qo00084j>

Scheme 1 OTC reactions, previous attempts and our proposed Au(I)/Rh(I) OTC.



In organometallic catalysis, many metal pairs have been studied, particularly those involving gold(i)⁵ or rhodium(i)⁶ in combination with another metal. Unexpectedly, no OTC procedure involving these two metals has yet been developed. Two attempts to combine them have been made, but they have failed. In 2013, Hashmi and Lautens developed a one-pot two-step procedure aimed at the enantioselective synthesis of β -functionalized ketones from propargyl alcohol derivatives (Scheme 1b).⁷

Unfortunately, the transposal of such a one-pot bimetallic procedure to the corresponding OTC procedure failed due to the over-functionalization process. In 2017, Yu provided a sequential procedure involving the Au(i)/Rh(i) couple toward the preparation of polycyclic molecules derivating from tetrahydroisoquinolinone. Attempts to add all components together from the start also failed (Scheme 1c).⁸

In this context, we aimed to develop an OTC procedure combining Au(i)-hydroacyloxylation and Rh(i)-hydroformylation reactions (Scheme 1d). For that purpose, we have selected substrate **1a** having an aryl moiety bearing an acid function and terminal alkyne, which can be transformed into the corresponding lactone **2a** by gold(i) catalysis. This latter feature an exocyclic double bond that is an appropriate target for undergoing functionalization *via* rhodium(i)-catalyzed hydroformylation. This sequence was considered because both reactions are highly efficient and would result in functionalized heterocyclic compounds.

Results and discussion

Before considering the OTC process, we have concentrated our effort on the optimization of each steps independently: the gold(i)-catalyzed hydroacyloxylation reaction, then the rhodium(i)-catalyzed hydroformylation reaction.

Our first objective was to carry out the hydroacyloxylation reaction under compatible conditions with an OTC procedure, *i.e.*, with simple conditions and the highest possible selectivity (Table 1).

Based on previously reported procedures for this transformation,⁹ the entire screening was conducted under the following conditions: substrate **1a** (1 equiv.), gold catalyst (1 mol%), possible additive (1 mol%), in dichloroethane (DCE, 0.25 M). We began by testing gold(i) chloride as catalyst.^{9a,b} We first used a phosphite gold(i) chloride (**Cat. A**) (entry 1), which failed to convert the substrate. However, when the cationic gold(i) complex is formed by the addition of silver hexafluoroantimonate (entry 2), substrate **1a** is completely converted into lactone **2a** within 15 minutes at room temperature. A full regioselectivity in favor of the 6-*endo*-dig cyclization was obtained as we never observed the formation of compound **3a** bearing the seven-membered ring. With the same conditions, the NHC-based **Cat. B** and **Cat. C** proved ineffective. Their reactivity was restored at 70 °C, albeit with a lower conversion for **Cat. B** (entries 3 and 4). In contrast, the reaction carried out in the presence of a pre-activated cationic gold(i) complex, the

Table 1 Optimization of the hydroacyloxylation reaction step^a

	CO ₂ H	[Au] (1 mol%)	
		DCE	
		RT/Time	
1a			2a + 3a
			Cat. A
			Cat. B
			Cat. C
			Cat. D

Entry	Catalyst	Time (min)	1a/2a ^c
1	Cat. A	60	100/0
2	Cat. A + AgSbF ₆	15	0/100
3 ^b	Cat. B + AgSbF ₆	60	60/40
4 ^b	Cat. C + AgSbF ₆	15	0/100
5	Cat. D	15	0/100

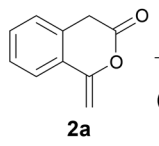
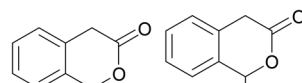
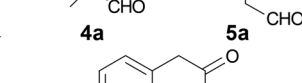
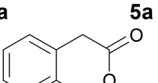
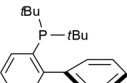
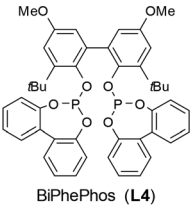
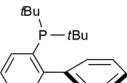
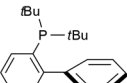
^a Reactions were performed by adding catalyst (1 mol%) to a solution of **1a** in DCE (0.25 M) at RT. ^b 70 °C. ^c Measured by ¹H NMR in the crude mixture.

commercially available catalyst $[(\text{JohnPhos})\text{Au}(\text{MeCN})][\text{SbF}_6]$ (**Cat. D**), leads to complete formation of **2a** without any additional additive within 15 minutes at room temperature (entry 5).

Once the hydroacyloxylation reaction was optimized, we investigated if it would be possible to apply the hydroformylation reaction to lactones **2a**. Indeed, the literature does not mention any example of the application of this transformation to such substrates. First, we determined the best ligand for the hydroformylation, the latter having a significant impact on the conversion of the reaction and its selectivity (Table 2). Three compounds can be obtained: iso-aldehyde **4a**, *n*-aldehyde **5a**, and compound **6a**, the latter resulting from the side hydrogenation reaction. This screening was carried out using lactone **2a** as substrate under reaction conditions commonly used: Rh (CO)₂(acac) (1 or 2 mol%), ligand **L** (1, 2 or 4 mol%) in toluene at 70 °C under the pressure of 20 bars of syngas (CO/H₂, 1 : 1).¹⁰ Monodentate phosphite ligands, such as P(OPh)₃ (**L3**), demonstrated better catalytic performance in the hydroformylation of **2a** than monodentate phosphine ligands, such as PPh₃ (**L1**) or JohnPhos (**L2**) (entries 1–3). On other side, bidentate phosphite ligands such as BiPhePhos (**L4**) did not allow a good conversion in **4a** (entry 4). We then explored various substituents on the aryl group of the monodentate phosphite ligands. Indeed, it is well established that the substitution pattern of aryl groups plays a key role in the activity and stability of the rhodium–phosphite complex.¹¹ An alkyl group in the *ortho* position improves the conversion to **4a** only minimally, if at all (**L5–L8**, entries 5–8). The ligand with a methoxy group in *para*-position (**L9**) was not performant at all, unlike



Table 2 Optimization of the hydroformylation reaction step^a

	$\xrightarrow{[\text{Rh}]/\text{L}}$ CO/H_2 $(1:1, 20 \text{ bars})$ Solvent $70^\circ\text{C}, 16\text{h}$	 4a	 5a
		 6a	
 JohnPhos (L2)	 BiPhePhos (L4)		$\xrightarrow{\text{Cat. D (1 mol\%)}}$ $[\text{Rh}](1 \text{ mol\%})$ $\text{L (2 mol\%})$ DCE, RT, 1 h
			2a

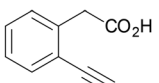
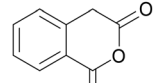
^a Reaction conditions: Rh(CO)₂(acac) (2 mol%), ligand (8 mol%), toluene.

^b Measured by ¹H NMR in the crude mixture. ^c Ligand (4 mol%). ^d Rh(CO)₂(acac) (2 mol%), **L10** (4 mol%), DCE. ^e Rh(CO)₂(acac) (1 mol%), **L10** (2 mol%), DCE.

the same group in *ortho*-position (**L10**) which gave an excellent result with 86% of conversion into **4a** (entries 9 and 10). The presence of the methoxy group in the *ortho*-position electronically enriches the aromatic ring, thereby enhancing the catalytic activity of the complex, while protecting the phosphorus atom against hydrolysis. We then decided to decrease the amount of ligand **L10** and to change the solvent of the reaction to DCE in order to standardize reaction conditions of the two transformations (hydroacyloxylation/hydroformylation). The result was exactly the same. This catalytic system was also efficient with the use of 1 mol% of Rh(CO)₂(acac) and 2 mol% of ligand **L10** (entry 12). It is noteworthy that during the development of the purification conditions of carbaldehyde **4a**, we found that it was unstable under both standard and reversed-phase chromatography conditions. Consequently, all the results presented in this part correspond to the conversions obtained by integrating the ¹H NMR spectrum of the crude reaction. Moreover, throughout the optimization of this reaction, we never observed the formation of the *n*-aldehyde **5a** or the hydrogenated substrate **6a**.

Since in the OTC procedure all catalytic species required must be present from the beginning, we studied the impact of the presence of ligand and rhodium(I) complex on the gold(I)-catalyzed hydroacyloxylation reaction (Table 3). We first observed that **Cat. D** $[(\text{L2})\text{Au}(\text{MeCN})][\text{SbF}_6]$, which has been identified as the most efficient catalyst to achieve regioselective

Table 3 Impact of **L10/Rh(CO)₂(acac)** on gold(I)-catalyzed hydroacyloxylation^a

 1a	$\xrightarrow{\text{Cat. D (1 mol\%)}}$ $[\text{Rh}](1 \text{ mol\%})$ $\text{L (2 mol\%})$ DCE, RT, 1 h	 2a
Entry	[Rh]	L
1	—	—
2	—	L10
3	Rh(CO) ₂ (acac)	L10

^a Measured by ¹H NMR in the crude mixture.

hydroacyloxylation of **2a**, loses its catalytic performance at room temperature after 1 h when it is placed in the presence of 2 equivalents of the **L10** ligand (entries 1 and 2). These results led us to hypothesize that in the presence of an excess of ligand, the loss of the catalytic performances of the gold(I) complex, could be related to the predominant formation of new organometallic species, $[(\text{L2})\text{Au}(\text{L10})][\text{SbF}_6]$, catalytically inert at room temperature in the hydroacyloxylation reaction. On the other hand, in the presence of ligand **L10**, when a rhodium(I) source is introduced into the reaction medium, we observe that the catalytic performances of the gold catalysts are regenerated (entry 3).

The presence of the rhodium(I) source could thus allow the release of a sufficient quantity of the catalytically active organo-gold species to complete the reaction. To confirm the possible interaction between **Cat. A**, Rh(CO)₂(acac), and ligand **L10**, we conducted a study by ³¹P NMR regarding several mixtures of the catalytic species involved at the beginning of our OTC procedure (Fig. 1).

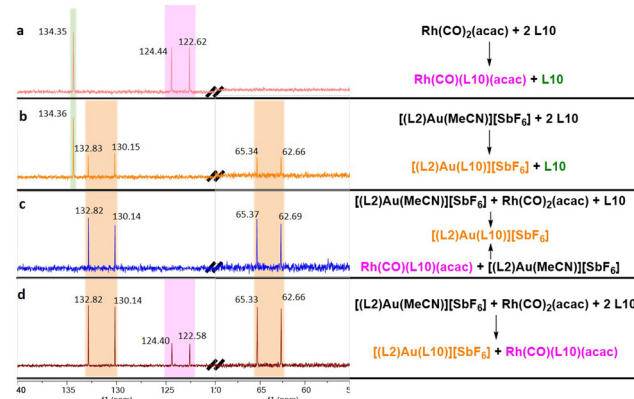


Fig. 1 ³¹P NMR analyses (162 MHz, CDCl₃) of different species involved in the OTC. Complete study and full spectrum are shown in ESI.† (a) Rh(CO)₂(acac) (1 equiv.), **L10** (2 equiv.), CDCl₃. (b) **Cat. D** (1 equiv.), **L10** (2 equiv.), CDCl₃. (c) Rh(CO)₂(acac) (1 equiv.), **Cat. D** (1 equiv.), **L10** (1 equiv.), CDCl₃ or Rh(CO)(L10)(acac) (1 equiv.), **Cat. D** (1 equiv.), CDCl₃. (d) Rh(CO)₂(acac) (1 equiv.), **Cat. D** (1 equiv.), **L10** (2 equiv.), CDCl₃.



We first characterized the rhodium pre-catalyst of our hydroformylation reaction, generated *in situ* by chelation of the commercial rhodium salt ($\text{Rh}(\text{CO})_2(\text{acac})$, 1 equiv.) by ligand **L10** (2 equiv.). This complex is characterized by a doublet at 123.53 ppm with a $^{31}\text{P}-^{103}\text{Rh}$ coupling constant of 293 Hz (spectrum a). It is interesting to note that the ligand **L10** was detected in the reaction medium in its free form (at 134.35 ppm) suggesting that the rhodium is bearing only one ligand ($\text{Rh}(\text{CO})(\text{L10})(\text{acac})$).¹² The ^{31}P NMR of **Cat. D**, shows one singlet at 57.02 ppm (not shown here, see ESI†) and the mixture of this catalyst with ligand **L10** shows two NMR signals (63.97 and 131.49 ppm) appearing as doublets due to a $^{31}\text{P}-^{31}\text{P}$ coupling ($J = 434$ Hz) through the gold atom, suggesting the formation of the $[(\text{L2})\text{Au}(\text{L10})][\text{SbF}_6]$ complex (spectrum b).¹³ These chemical shifts were used as a reference to study the affinity of ligand **L10** in the presence of the bimetallic couple $\text{Au}(\text{i})/\text{Rh}(\text{i})$. Indeed, when ligand **L10** (1 equiv.) is added to a mixture of the two metallic species (1 equiv. each), we have observed the appearance in ^{31}P NMR of the characteristic signal of the $[(\text{L2})\text{Au}(\text{L10})][\text{SbF}_6]$ complex (spectrum c). This observation shows that ligand **L10** has a greater affinity for $\text{Au}(\text{i})$ than $\text{Rh}(\text{i})$. The same result is observed if $\text{Au}(\text{i})$ (1 equiv.) is added into a mixture of $\text{Rh}(\text{i})$ (1 equiv.) and ligand **L10** (1 equiv., spectrum c), confirming a weaker binding force between the ligand and $\text{Rh}(\text{i})$. The last experience shows an equimolar distribution of the ligand **L10**, in case of using 2 equiv. of **L10** facing to one equivalent of each metal (spectrum d). It is important to note that the ligand JohnPhos (**L2**) was never detected in the reaction medium, either in its free form or in the form of complex $\text{Rh}(\text{i})$ -JohnPhos, inactive in the hydroformylation reaction applied to our heterocycles (*cf.* Table 2, entry 2). In order to evaluate the potential impact of syngas on the complexation of **L10** with the gold complex, we bubbled syngas through a solution containing $\text{Au}(\text{i})$ and **L10** in a 1:2 ratio. No change was observed, and the obtained spectrum was identical to spectrum b (Fig. 1). One equivalent of $\text{Rh}(\text{i})$ was subsequently added, and the recorded spectrum remained identical to spectrum d (Fig. 1). All these experiments only provide an insight into the initial state of the catalytic system in the OTC. We then focused the study on the $\text{Au}(\text{i})/\text{Rh}(\text{i})$ OTC reaction, thus, seeking to find a compatibility between the two organometallic systems. In this regard, we have combined the reaction conditions as the best for either of the transformations involved. The objective was the formation of the carbaldehyde of interest **4a**, by adding **Cat. D** (1 mol%) to a solution of 2-(2-ethynylphenyl)acetic acid **1a**, $\text{Rh}(\text{CO})_2(\text{acac})$ (1 mol%) and $\text{P}(\text{2-MeOPhO})_3$ (**L10**, 2 mol%) in DCE at 70 °C under the pressure of 20 bars of syngas (Table 4, entry 1).

The combination of the two previously optimized reaction conditions (1 mol% of **Cat. D** and $\text{Rh}(\text{CO})_2(\text{acac})$ and 2 mol% of **L10**) allowed a total conversion of acid **1a**, the acquisition of carbaldehyde **4a** with a conversion of 84%, and further information on the composition of the crude of reaction of such a transformation. We observed residual traces of intermediate lactone **2a** (9%) and identified three secondary products. Aldehydes **8a** and **9a** are derived from over-functionalization,

Table 4 OTC optimization^{a,b}

Entry	x	y	z	4a	2a	7a	8a/9a
				84	9	2	5
1	1	1	2	84	9	2	5
2	0	1	2	0	11	0	89
3	1	0	2	0	100	0	0
4	1	1	0	2	94	2	2
5	1	1	2	2	84	3	11
6	1	2	4	84	3	3	10
7	1	4	4	90	5	0	5

^a Reaction conditions: **Cat. D** (x mol%), $\text{Rh}(\text{CO})_2(\text{acac})$ (y mol%), **L10** (z mol%), DCE (0.25 M), CO/H_2 (1:1, 20 bars), 70 °C, 16 h. ^b Ratio measured by ^1H NMR in the crude mixture.

which arises directly from the presence of reactive species from the initial moment of the procedure. Here, this phenomenon takes the form of a hydroformylation-reduction reaction applied directly to the unsaturation of 2-(2-ethynylphenyl)acetic acid **1a**.¹⁴ The acetophenone **7a** derived from the hydrolysis of lactone intermediate **2a**. Moreover, as expected, without gold catalyst, product **8a** and **9a** from hydroformylation-reduction reaction were mostly recovered with little part of **2a** showing that $\text{Rh}(\text{i})$ was able to catalyze hydroacyloxylation but not as fast as the hydroformylation reaction (entry 2). Without $\text{Rh}(\text{i})$ catalyst, only **2a** was recovered (entry 3) and without **L10** the hydroformylation reaction was not efficient at all (entry 4).

With these reaction conditions in hand, **Cat. D** (1 mol%), $\text{Rh}(\text{CO})_2(\text{acac})$ (1 mol%), **L10** (2 mol%), DCE (0.25 M), CO/H_2 (1:1, 20 bars), 70 °C, we studied the kinetic of this OTC (Fig. 2).

When the OTC reaction was stopped after 1 h, 97% of the starting substrate **1a** has been converted into **2a**, without formation of product **4a** (Fig. 2, red and blue plained curves). This is comparable with the rate of hydroacyloxylation reaction of **1a** (Fig. 2, dashed red curve). After 4 h, the OTC reaction does not seem to have evolved much, the starting substrate **1a** is still not completely consumed and only 2% of the expected product **4a** is formed. After 8 h of reaction, the substrate is completely converted. The desired product proportion **4a** has reached 6% conversion. After 10 h of reaction, the results observed have hardly changed, indicating little progress in the OTC between 1 h and 10 h. The progress of the reaction increases sharply from 10 h onwards. Indeed, the conversion

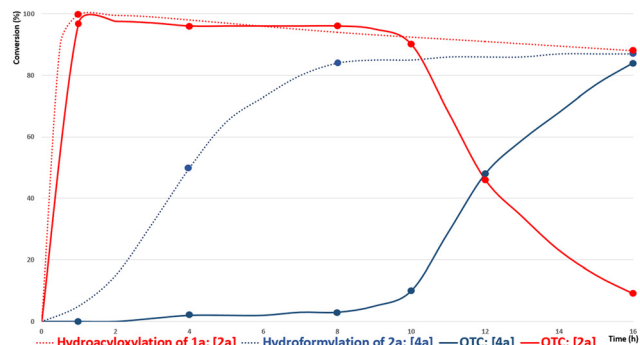


Fig. 2 Kinetic study of $[\text{Au(i)}]/[\text{Rh(i)}]$ OTC reaction of **1a**. Red and blue plained curves, OTC reaction, conditions: **Cat. D** (1 mol%), $\text{Rh}(\text{CO})_2(\text{acac})$ (1 mol%), **L10** (2 mol%), DCE (0.25 M), CO/H_2 (1:1, 20 bars), 70 °C. Dashed red curve, hydroacyloxylation of **1a**, conditions: **Cat. D** (1 mol%), DCE, RT. Dashed blue curve, hydroformylation of **2a**, conditions: $\text{Rh}(\text{CO})_2(\text{acac})$ (1 mol%), **L10** (2 mol%), DCE (0.25 M), CO/H_2 (1:1, 20 bars), 70 °C, 16 h.

of **2a** into **4a** reached 48%, at 12 h suggesting that Rh(i) hydroformylation takes place from the 10 h threshold. After 16 h, the reaction is almost complete, with only 9% of product **2a** remaining. Compared to the hydroformylation of **2a** (Fig. 2, blue dashed curves), only 4 h is necessary to reach 50% conversion into **4a** and 8 h for the completion of the reaction. Moreover, under these reaction conditions, the OTC reaction proved to be non-reproducible, with the lactone **2a** as the major products (Table 4, entries 1 and 5). The slowdown of the hydroformylation reaction, combined with the lack of reproducibility of the OTC reaction, led us to double the amount of rhodium complex and ligand (respectively 2 and 4 mol%, entry 6).

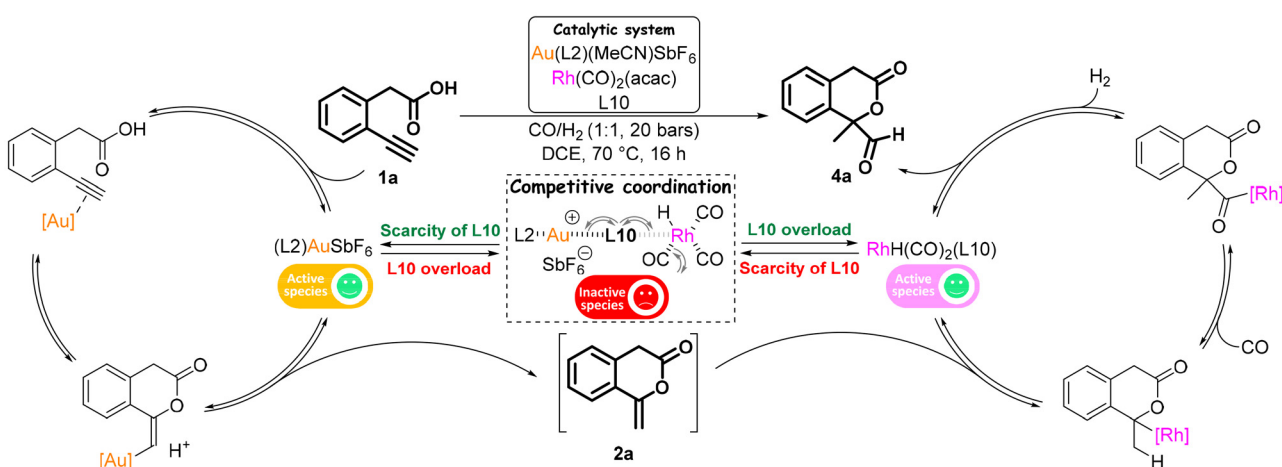
This restored good conversion to the targeted aldehyde **4a**, but also favored the hydroformylation of **1a** over its hydroacyloxylation, as 10% of aldehydes **8a/9a** is recovered. Therefore, we then increased the quantity of rhodium to 4 mol% to limit the amount of free **L10** (Table 4, entry 7). In this way, we succeed to obtain carbaldehyde **4a** with a conversion of 90%

and good reproducibility. Eventually, the use of **Cat. D** (1 mol%), $\text{Rh}(\text{CO})_2(\text{acac})$ (4 mol%) and **L10** (4 mol%) in DCE (0.25 M) under syngas pressure (20 bars) at 70 °C proved to be the conditions of choice for this OTC reaction.

Based on competitive ligand coordination between the two metal complexes, we propose the mechanism detailed in Scheme 2 for this $\text{Au(i)}/\text{Rh(i)}$ OTC. As shown by experiments on interactions between catalytic systems, as well as the kinetic study performed on the OTC, competitive ligand coordination between the gold and rhodium catalysts lead to their partial and reversible deactivations. On the one hand, at the beginning of the reaction, since ligand **L10** coordinates more easily gold than rhodium, an equilibrium is established. A low amount of **L10** facilitates its decoordination from gold in favor of substrate **1a**. **L10** can then be intercepted by rhodium and the hydroacyloxylation reaction can take place. After proton-deauration, lactone **2a** is formed. On the other hand, the bimetallic equilibrium would also allow the formation of the active rhodium complex bearing only one ligand **L10**, through competitive coordination with the gold complex. At this stage, a sufficient amount of both Rh(i) complex and **L10** are necessary to promote the hydroformylation reaction. If so, this allows the reaction of lactone **2a** with the rhodium complex, which, after carbon monoxide insertion, dihydrogen addition, and reductive elimination, would yield aldehyde **4a**.

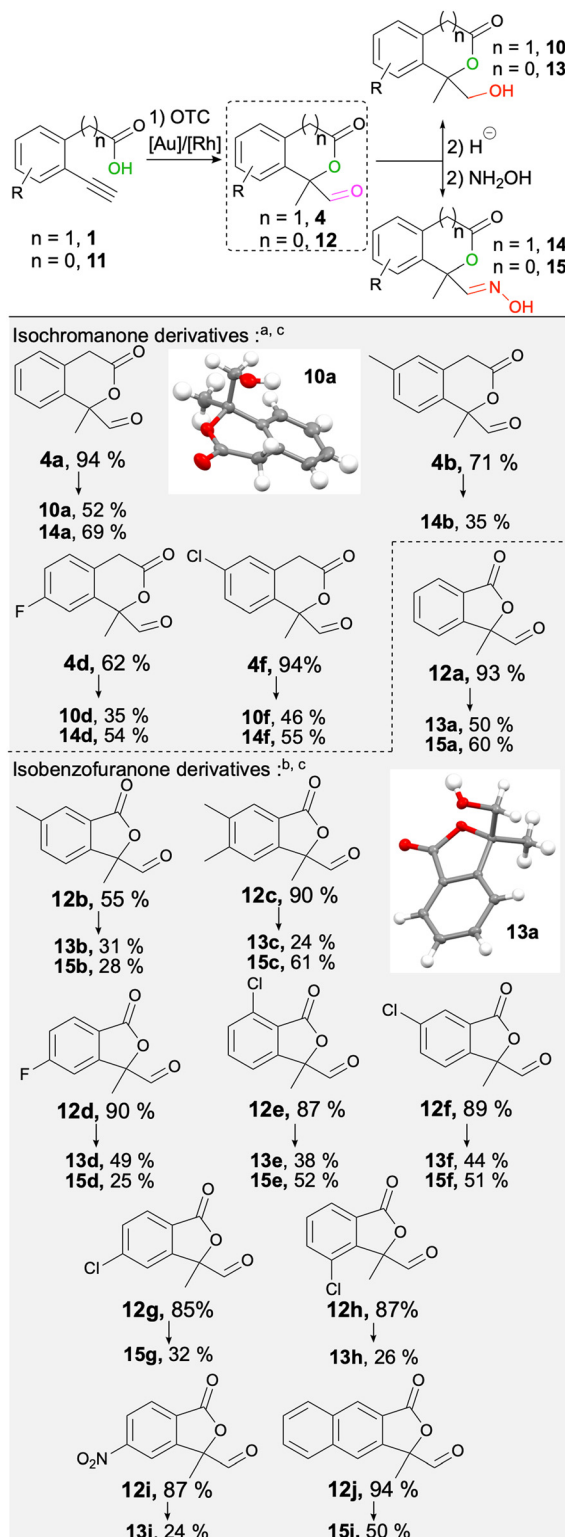
Then, we explored the scope of the reaction. As illustrated in Scheme 3, the OTC transformation is efficient on a broad range of substrate **1** with good to excellent conversions in favor of aldehydes **4** (55–94%). As in case of **1a**, all of these transformations proved remarkably regioselective as only one compound was obtained in each case. A wide range of aryls exhibiting electron-donating or withdrawing groups are well tolerated at any position without affecting the conversion (for example compounds **12e–h**).

As discussed above, due to the inherent instability of the various carbaldehydes obtained, we have developed several derivatization reactions to be applied at the end of the $\text{Au(i)}/\text{Rh(i)}$ OTC procedure to obtain sufficiently stable compounds to



Scheme 2 Proposed mechanism of the $\text{Au(i)}/\text{Rh(i)}$ OTC reaction from **1a** to **4a**.





Scheme 3 Au(I)-hydroacyloxylation/Rh(I)-hydroformylation OTC followed with derivatization reactions. ^a (1) Cat. D (1 mol%), Rh(CO)₂(acac) (4 mol%), L10 (4 mol%), DCE (0.25 M), CO/H₂ (1:1, 20 bars), 70 °C, (2) NaBH₃CN (2 equiv.), DCM, RT, 16 h. ^b (1) Cat. D (1 mol%), Rh(CO)₂(acac) (4 mol%), L10 (4 mol%), DCE (0.25 M), CO/H₂ (1:1, 20 bars), 70 °C, (2) NaBH₄ (2 equiv.), MeOH, RT, 16 h. ^c (1) Cat. D (1 mol%), Rh(CO)₂(acac) (4 mol%), L10 (4 mol%), DCE (0.25 M), CO/H₂ (1:1, 20 bars), 70 °C, (2) NaOAc (2 equiv.), NH₂OH-HCl (2 equiv.), EtOH, RT, 16 h.

be isolated and characterized. First, we focused on the classical reduction of aldehydes in the corresponding primary alcohol (compounds **10** and **13**, Scheme 3). For this, we performed a screening of different reduction systems (NaBH₄, NaBH₃CN, NaBH(OAc)₃, DIBAL-H). It appeared that the best conditions to transform carbaldehydes **4** into alcohols **10** was the use of NaBH₃CN in DCM, while for the transformation of carbaldehydes **11** into **13**, it was the use of NaBH₄ in MeOH. The application of the OTC procedure Au(I)/Rh(I) hydroacyloxylation/hydroformylation followed by the reduction reaction allowed the preparation of 11 heterocycles **10** and **13** with yields ranging from 24 to 52%. The structures of two compounds were confirmed by crystallization: compound **10a** and **13a**.

A second derivatization reaction have been developed. We were interested in the condensation of carbaldehydes **4** and **12** with hydroxylamine to give the corresponding oximes **14** and **15** (Scheme 3). The crude mixture from the OTC reaction was thus directly solubilized in ethanol, and sodium acetate and hydroxylammonium chloride were added. The application of the OTC/hydroxylamine condensation procedure allowed the preparation of 12 new heterocycles bearing an oxime moiety with yields ranging from 25 to 69%. These yields are, for the most part, closer to the conversions observed after the OTC procedure than those obtained with the previous derivatization.

Conclusion

In summary, we have developed an orthogonal tandem catalysis involving Au(I)-hydroacyloxylation and Rh(I)-hydroformylation, demonstrating that these two metals are compatible with each other. The application of the Au(I)/Rh(I) hydroacyloxylation/hydroformylation OTC procedure gave access to 14 carbaldehydes of interest. After derivatization reactions, 11 alcohols and 12 oximes were obtained, with yields ranging from 24 to 52% and from 25 to 69%, respectively. ³¹P NMR experiments and a kinetic study carried out on the OTC allowed a detailed understanding of the catalytic cycles involved, highlighting the competitive ligand coordination between the gold and rhodium catalysts. These studies allowed for the determination of the optimal catalytic conditions, leading to the development of the first OTC Au(I)/Rh(I) reaction.

Author contributions

The manuscript was written through contributions of all authors. All authors have given approval to the final version of the manuscript.

Data availability

All the data are available in the ESI† including ¹H, ¹³C, ³¹P and ¹⁹F description and spectra.



The data for **10a** and **13a** will be provided when this article is accepted. CCDC 2384274 for **10a** and 2111415[†] for **13a** contains the supplementary crystallographic data for this paper.

A checkcif is provided in the list of documents supplied for compounds **10a** and **13a**.

Conflicts of interest

There are no conflicts to declare.

Acknowledgements

This work of the Interdisciplinary Thematic Institute InnoVec, as part of the ITI 2021-2028 program of the University of Strasbourg, CNRS and Inserm, was supported by IdEx Unistra (ANR-10-IDEX-0002) and SFRI (STRAT'US project) under the framework of the French Investments for the Future Program. The doctoral grant for E.S. was financed by the “Ministère de l'Enseignement Supérieur, de la Recherche et de l'Innovation”. We thank the leading committee of our laboratory (LIT, UMR 7200) for the technical support, the platform PACSI (GDS 3670) for NMR and mass analyses and Lydia Karmazin and Corinne Bailly (GDS 3648) for X-ray analyses.

References

- 1 S. Martínez, L. Veth, B. Lainer and P. Dydio, Challenges and Opportunities in Multicatalysis, *ACS Catal.*, 2021, **11**, 3891–3915.
- 2 (a) F. Romiti, J. Del Pozo, P. H. S. Paioti, S. A. Gonsales, X. Li, F. W. W. Hartrampf and A. H. Hoveyda, Different Strategies for Designing Dual-Catalytic Enantioselective Processes: From Fully Cooperative to Non-Cooperative Systems, *J. Am. Chem. Soc.*, 2019, **141**, 17952–17961; (b) S. Afewerki and A. Córdova, Combinations of Aminocatalysts and Metal Catalysts: A Powerful Cooperative Approach in Selective Organic Synthesis, *Chem. Rev.*, 2016, **116**, 13512–13570; (c) A. E. Allen and D. W. C. MacMillan, Synergistic Catalysis: A Powerful Synthetic Strategy for New Reaction Development, *Chem. Sci.*, 2012, **3**, 633.
- 3 T. L. Lohr and T. J. Marks, Orthogonal Tandem Catalysis, *Nat. Chem.*, 2015, **7**, 477–482.
- 4 S. Biswas, B. F. Van Steijvoort, M. Waeterschoot, N. R. Bheemireddy, G. Evano and B. U. W. Maes, Expedient Synthesis of Bridged Bicyclic Nitrogen Scaffolds via Orthogonal Tandem Catalysis, *Angew. Chem., Int. Ed.*, 2021, **60**, 21988–21996.
- 5 (a) P. García-Domínguez and C. Nevado, Au–Pd Bimetallic Catalysis: The Importance of Anionic Ligands in Catalyst Speciation, *J. Am. Chem. Soc.*, 2016, **138**, 3266–3269; (b) S. Ge, W. Cao, T. Kang, B. Hu, H. Zhang, Z. Su, X. Liu and X. Feng, Bimetallic Catalytic Asymmetric Tandem Reaction of β -Alkynyl Ketones to Synthesize 6,6-Spiroketals, *Angew. Chem., Int. Ed.*, 2019, **58**, 4017–4021; (c) S. Ge, Y. Zhang, Z. Tan, D. Li, S. Dong, X. Liu and X. Feng, Bimetallic Catalytic Tandem Reaction of Acyclic Enynes: Enantioselective Access to Tetrahydrobenzofuran Derivatives, *Org. Lett.*, 2020, **22**, 3551–3556; (d) J. Li, L. Lin, B. Hu, X. Lian, G. Wang, X. Liu and X. Feng, Bimetallic Gold(i)/Chiral *N,N'*-Dioxide Nickel (ii) Asymmetric Relay Catalysis: Chemo- and Enantioselective Synthesis of Spiroketals and Spiroaminals, *Angew. Chem., Int. Ed.*, 2016, **55**, 6075–6078; (e) M. Al-Amin, K. E. Roth and S. A. Blum, Mechanistic Studies of Gold and Palladium Cooperative Dual-Catalytic Cross-Coupling Systems, *ACS Catal.*, 2014, **4**, 622–629; (f) M. Al-Amin, J. S. Johnson and S. A. Blum, Selectivity, Compatibility, Downstream Functionalization, and Silver Effect in the Gold and Palladium Dual-Catalytic Synthesis of Lactones, *Organometallics*, 2014, **33**, 5448–5456; (g) S. Biswas, R. A. Watile and J. S. M. Samec, Tandem Pd/Au-Catalyzed Route to α -Sulfonylated Carbonyl Compounds from Terminal Propargylic Alcohols and Thiols, *Chem. – Eur. J.*, 2014, **20**, 2159–2163; (h) H. Wu, Y. He and L. Gong, The Combination of Relay and Cooperative Catalysis with a Gold/Palladium/Brønsted Acid Ternary System for the Cascade Hydroamination/Allylic Alkylation Reaction, *Adv. Synth. Catal.*, 2012, **354**, 975–980.
- 6 (a) M. M. Lorion, K. Maindan, A. R. Kapdi and L. Ackermann, The Combination of Relay and Cooperative Catalysis with a Gold/Palladium/Brønsted Acid Ternary System for the Cascade Hydroamination/Allylic Alkylation Reaction, *Chem. Soc. Rev.*, 2017, **46**, 7399–7420; (b) T. Gaide, J. Bianga, K. Schlipkötter, A. Behr and A. J. Vorholt, Linear Selective Isomerization/Hydroformylation of Unsaturated Fatty Acid Methyl Esters: A Bimetallic Approach, *ACS Catal.*, 2017, **7**, 4163–4171; (c) S. Fuchs, T. Rösler, B. Grabe, A. Kampwerth, G. Meier, H. Strutz, A. Behr and A. J. Vorholt, Synthesis of Primary Amines via Linkage of Hydroaminomethylation of Olefins and Splitting of Secondary Amines, *Appl. Catal. A*, 2018, **550**, 198–205; (d) M. R. L. Furst, V. Korkmaz, T. Gaide, T. Seidensticker, A. Behr and A. J. Vorholt, Tandem Reductive Hydroformylation of Castor Oil Derived Substrates and Catalyst Recycling by Selective Product Crystallization, *ChemCatChem*, 2017, **9**, 4319–4323.
- 7 M. M. Hansmann, A. S. K. Hashmi and M. Lautens, Gold Meets Rhodium: Tandem One-Pot Synthesis of β -Disubstituted Ketones via Meyer-Schuster Rearrangement and Asymmetric 1,4-Addition, *Org. Lett.*, 2013, **15**, 3226–3229.
- 8 Z. Zhuang, C.-L. Li, Y. Xiang, Y.-H. Wang and Z.-X. Yu, An Enyne Cycloisomerization/[5 + 1] Reaction Sequence to Synthesize Tetrahydroisoquinolinones from Enyne-Enes and CO, *Chem. Commun.*, 2017, **53**, 2158–2161.
- 9 (a) E. Marchal, P. Uriac, B. Legouin, L. Toupet and P. V. D. Weghe, Cycloisomerization of γ - and δ -Acetylenic Acids Catalyzed by Gold(i) Chloride, *Tetrahedron*, 2007, **63**, 9979–9990; (b) E. Genin, P. Y. Toullec, S. Antoniotti, C. Brancour, J.-P. Genêt and V. Michelet, Room



- Temperature Au(i)-Catalyzed *Exo*-Selective Cycloisomerization of Acetylenic Acids: An Entry to Functionalized γ -Lactones, *J. Am. Chem. Soc.*, 2006, **128**, 3112–3113; (c) R. Nolla-Saltiel, E. Robles-Marín and S. Porcel, Silver(i) and Gold(i)-Promoted Synthesis of Alkylidene Lactones and 2H-Chromenes from Salicylic and Anthranilic Acid Derivatives, *Tetrahedron Lett.*, 2014, **55**, 4484–4488.
- 10 L. Salacz, C. Charpentier, J. Suffert and N. Girard, Desymmetrizing Hydroformylation of Dihydromuconic Acid Diesters: Application to the Synthesis of (\pm) -Vindeburnol, *J. Org. Chem.*, 2017, **82**, 2257–2262.
- 11 S. Kloß, D. Selent, A. Spannenberg, R. Franke, A. Börner and M. Sharif, Effects of Substitution Pattern in Phosphite Ligands Used in Rhodium-Catalyzed Hydroformylation on Reactivity and Hydrolysis Stability, *Catalysts*, 2019, **9**, 1036.
- 12 A. Bara-Estaún, C. L. Lyall, J. P. Lowe, P. G. Pringle, P. C. J. Kamer, R. Franke and U. Hintermair, Understanding Rh-catalysed Hydroformylation with Phosphite Ligands through Catalyst Speciation Analysis by *Operando* FlowNMR Spectroscopy, *ChemCatChem*, 2023, **15**, e202201204.
- 13 A. Zhdanko, M. Ströbele and M. E. Maier, Coordination Chemistry of Gold Catalysts in Solution: A Detailed NMR Study, *Chem. – Eur. J.*, 2012, **18**, 14732–14744.
- 14 C. Botteghi and C. Salomon, Conclusive Evidence for Direct Hydroformylation of the Triple Bond Catalyzed by Chiral Rhodium-Complexes, *Tetrahedron Lett.*, 1974, **15**, 4285–4288.